Desalination and Water Treatment
www.deswater.com

doi: 10.1080/19443994.2015.1005689

57 (2016) 6268–6277
March

Taylor & Francis
Taylor & Francis Group

Kinetic studies on novel cation exchangers, antimony zirconium phosphate (SbZP) and antimony zirconium triethylammonium phosphate (SbZTP)

B. Preetha[a,b,*], C. Janardanan[b]

[a]*Department of Chemistry, University College, Thiruvananthapuram 695034, Kerala, India, Tel. +91 9446097226; email: preethaba@gmail.com*
[b]*Post Graduate and Research Department of Chemistry, Sree Narayana College, Thottada P. O., Kannur 670 007, Kerala, India, Tel. +91 9846097548; email: jeeje_dianthus@yahoo.com (C. Janardanan)*

Received 9 May 2014; Accepted 4 January 2015

ABSTRACT

Some of the important features of ion exchangers based on antimony(III) are that they have high capacities and the capacities are retained even at high temperatures. Ion-exchange kinetic studies of metal ions on newly synthesised antimony zirconium phosphate and antimony zirconium triethylammonium phosphate were carried out under particle diffusion controlled conditions. Exchange kinetics of Zn^{2+}, Mg^{2+} and Ca^{2+} has been studied, and a mechanism of exchange proposed. Various kinetic parameters such as pre-exponential constant (D_o), energy of activation (E_o) and entropy of activation (ΔS^*) were evaluated which showed the feasibility of metal ion exchange with H^+ ions on these materials. D_o gives an idea about the mobility of migrating ions. It depends on size and charge of ions, electrostatic interaction of metal ions with exchange sites, site acidity, pore size of exchanger particles, etc. The negative values of ΔS^* indicate that the exchange process by metal ions is feasible on the H^+ form of the material. Thus, we can predict the feasibility of an ion-exchange process to be used as a catalyst or inhibitor. The two exchangers under study showed similar trend in kinetic parameters. Their ion-exchange capacities could explain the different values of kinetic parameters obtained.

Keywords: Ion exchange; Composite; Diffusion; Exchange capacity; Kinetic parameters

1. Introduction

Recent technologies in the synthesis of ion-exchange materials were attempted to find new materials with structure suitable for many purposes. Growing environmental problems have also necessitated the selective determination and removal of metal ions, for which inorganic ion exchangers are found to be suitable. Novel composites using combinations of various ion exchangers are also being investigated. Although a lot of work has already been done on the synthesis of inorganic ion exchangers, the development of new inorganic ion exchangers with characteristic properties still needed attention and their utility in various fields is yet to be explored. A number of phosphate containing ion exchangers were reported and studied. Amorphous zirconium phosphate, an inorganic ion exchangers was synthesised by sol–gel method and sorption/ion-exchange behaviour of metal ions, Pb(II), Bi(III) and Th(IV) towards it were studied by varying the temperature, kinetic (over all

---

*Corresponding author.

rate constant, equilibrium constant) and thermodynamic parameters such as ΔG°, ΔH° and ΔS° were evaluated and adsorption isotherms (Langmuir and Fruendlich) studied [1]. Electrical conductivity and ion-exchange kinetic studies of polythiophene Sn(VI) phosphate nano-composite cation-exchanger [2] and cation mobility and kinetics of ion-exchange in zirconium hydrogen monothiophosphate hydrate [3] were also reported. Some of the important features of ion exchangers based on zirconium(IV) and antimony(III) are that they have high capacities and the capacities are retained even at high temperatures [4] Inorganic–organic composite materials were reported to show improved properties. So the present work deals with the synthesis and properties of antimony zirconium phosphate (SbZP) and antimony zirconium triethylammonium phosphate (SbZTP).

Ion exchangers find applications in heterogeneous catalysis, protective coatings, ion selective electrodes, ion-exchange membranes, biosensors, etc. Studies on kinetics of exchange enable us to understand the viability of an ion-exchange material in these fields. Kinetic studies on the ion exchangers are useful for predicting the ion-exchange process occurring on the surface of the exchanger. Kinetic studies envisage the three aspects of ion-exchange process, viz, the mechanism of ion exchange, rate determining step and the rate laws obeyed by the ion-exchange system. The Nernst–Planck equations with some additional assumptions provide appropriate values in obtaining the values of the various kinetic parameters precisely [5].

In the present work, exchange kinetics of three cations showing a common oxidation state of +2, Zn^{2+}, Mg^{2+} and Ca^{2+} with H^+ ions on the exchangers is studied. Zn^{2+} is similar to Mg^{2+} in chemical properties and size. Based on the studies, a mechanism of exchange is proposed. Various kinetic parameters such as pre-exponential constant (D_o), energy of activation (E_o) and entropy of activation (ΔS^*) are evaluated.

2. Experimental

2.1. Synthesis and characterisation of ion exchangers

SbZP was prepared by adding sodium dihydrogen phosphate solution to a solution mixture of zirconium oxychloride and antimony chloride (0.05 M each) in different volume ratios at a pH of 0.5 at 30˚C. SbZTP was prepared by adding triethylammonium phosphate solution to a mixture of antimony chloride and zirconium oxychloride solutions (0.05 M each) in different volume ratios at a pH of 2 at 30˚C. The total volume is limited to 500 ml. The product obtained in each case was stirred well and kept for 24 h at room temperature. The pH was adjusted using dilute nitric acid/sodium hydroxide solutions. The precipitate so obtained was filtered and washed several times with distilled water until the filtrate was free from acid. The dried materials were converted into H^+ form by immersing in 1.0 M HNO_3 with intermittent shaking and changing of acid. It was sieved to required mesh size. The exchanger was stored over ammonium chloride in desiccators to maintain certain amount of humidity.

Zirconium was analysed gravimetrically by fusing 0.1 g of the well-powdered ion exchanger with 1:1 mixture of K_2CO_3 and Na_2CO_3 and extracting with hot demineralised water. The undissolved portion was ignited and weighed as ZrO_2. Antimony and phosphate were determined by dissolving 0.1 g of the exchanger in hot concentrated mineral acid and making up to 100 ml. From this, antimony was estimated by pyrogallate method and phosphate as ammonium molybdophosphate [6]. Percentage of nitrogen was determined using CHN analyser. Elemental composition was also confirmed from energy dispersive X-ray spectrum of the samples.

Ion-exchange capacity (IEC) of the material was determined by column method. A glass column of 25 cm long and 1.0 cm in diameter having a stopcock and a porous disk of glass wool at the bottom was used as column. One gram of the exchanger in H^+ form was taken in the column. The H^+ ions were eluted by percolating 100 ml of 1 M sodium chloride solution at the rate of 5–6 drops per minute. The eluent was collected and titrated against standard sodium hydroxide solution. IEC as milli-equivalents of H^+ ions per gram was calculated from the titre values.

SbZP of highest sodium IEC of 0.85 meq/g, prepared from antimony chloride, zirconium oxychloride and sodium dihydrogen phosphate in the ratio of 2:1:2, appeared as colourless glassy solid, and the SbZTP sample with the highest exchange capacity of 1.2 meq/g, prepared from antimony chloride, zirconium oxychloride and triethylammonium phosphate in the ratio of 2:1:4, appeared as light brownish yellow coloured glassy solid. These were selected for detailed studies.

Distribution studies were carried out for various metal ions in demineralised water by batch process. In this method, 0.1 g of the exchanger (60–100 mesh) was equilibrated with 20 ml of the metal ion solutions for 24 h at room temperature. The metal ion concentrations before and after sorption were determined spectrophotometrically or by complexometric titration against standard EDTA solution. Distribution coefficients of metal ions were calculated which is the ratio of the concentration of the metal ion in the ion exchanger to that in the solution.

Various spectroscopic methods were also used for the characterisation of the materials. UV–visible spectrophotometer model JASCO V660 with diffuse reflectance accessory (integrated sphere) was used for spectrophotometric measurements. FT-IR spectrometer model Thermo-Nicolet Avtar 370 for IR studies, X-ray diffractometer Bruker AXS D8 advance for X-ray diffraction studies, Perkin–Elmer Diamond TG/DTA analysis system for thermal analysis and Quantachrome NOVA automated gas sorption system for BET surface area analysis were used.

2.2. Kinetic studies

Kinetic measurements were carried out by limited batch technique. In this technique, 20 ml fractions of 0.01 M metal ion solutions were shaken with 200 mg of the exchanger in several stoppered bottles at different temperatures (30, 45 and 52°C) for different time intervals (1, 2, 3, 4 and 5 min). The supernatant liquid was removed immediately and titrated against standard EDTA solution to determine the concentration of metal ions. Each set was repeated three times, the mean values were taken, and various kinetic parameters were evaluated.

Equilibrium experiments were performed by shaking 200 mg of exchanger particles at desired temperatures (30, 45 and 52°C) in a shaker bath for 6 h. After equilibrium, supernatant was removed and metal ion content was estimated by EDTA titration.

3. Results and discussion

3.1. Characterisation of SbZP and SbZTP

Chemical analysis of the samples showed the ratio of Sb, Zr and P as 2:1:2 in SbZP and Sb, Zr, triethylammonium and P as 2:1:2:2 in SbZTP.

The materials were found to be quite stable in lower concentrations of mineral acids such as 1.0 M HNO_3, 1.0 M H_2SO_4 and 1.0 M HCl, 0.01 M solutions of bases and organic solvents such as ethanol, acetone and carbon tetrachloride.

TGA analysis of SbZP (Fig. 1) shows 25% loss of weight due to the evaporation of water of hydration and condensation of structural hydroxyl groups. The evaporation of external water molecules is confirmed from the endothermic peak at 100°C. Above this temperature, a slight change in weight is observed. Above 600°C, some degradation takes place which is accompanied by weight loss and energy changes. Thus, thermo-gravimetric analysis clearly reveals that the sample is quite stable at high temperatures up to 600°C and can be used for high-temperature applications. TGA of SbZTP (Fig. 2) shows evaporation of water of hydration at 100°C which is revealed by the weight loss and the presence of endothermic peak. A total weight loss of 22% takes place. Thereafter, up to 450°C, no noticeable weight change or phase changes or heat flow was observed which gets confirmed from DTG also. This high stability of the material is a characteristic property required for ion exchangers. Thus, the exchanger can be used for high-temperature applications. After 450°C, the material shows sharp changes in weight due to decomposition.

FTIR spectrum of the materials (Figs. 3 and 4) shows broad bands in the region ~3,450 cm^{-1} which are attributed to symmetric and asymmetric –OH stretching, while the band at ~1,630 cm^{-1} is attributed to H–O–H bending. A band in the region ~1,384 cm^{-1} is attributed to the presence of δ (POH) indicating the presence of structural hydroxyl protons in SbZP, which is more evident from the obtained IEC values, and the band at ~1,051 and ~1,042 cm^{-1} is attributed to P=O stretching. Bands below 500 cm^{-1} show the presence of metal-oxygen bonds [7,8].

Based on chemical composition, TGA data and IR studies the tentative mixed oxide formula suggested for SbZP and SbZTP are $Sb_2O_3{\cdot}ZrO_2{\cdot}P_2O_5{\cdot}10.5H_2O$ and $Sb_2O_3{\cdot}ZrO_2{\cdot}(C_2H_5)_3N\ P_2O_5{\cdot}9H_2O$, respectively. The number of water molecules (n) was determined using Alberti–Torroca formula [9],

$$18n = \frac{x(M + 18n)}{100} \tag{1}$$

where x is the percentage of water content and $(M + 18n)$ is the molar mass of the material. The number of water molecules includes that due to condensation of structural hydroxyl groups, XRD pattern shows amorphous nature for SbZP and some peaks of very low intensities with one at $2\theta = 26.87^\circ$ for SbZTP showing very low crystalline character.

SEM analysis shows granular nature of the materials formed by agglomeration of particles which makes it suitable for column operations. Porous nature also increases the surface area.

BET surface area analyses show relatively high surface areas of 258 and 210 m^2/g for SbZP and SbZTP, respectively, which increases their catalytic activities.

UV–visible diffuse reflectance spectrum shows absorption edge in the UV region at about 300 nm.

pH titration curves show mono-functional nature for SbZP and bi-functional nature for SbZTP. The ion-exchange capacities obtained from the curves are in agreement with that obtained by the column method.

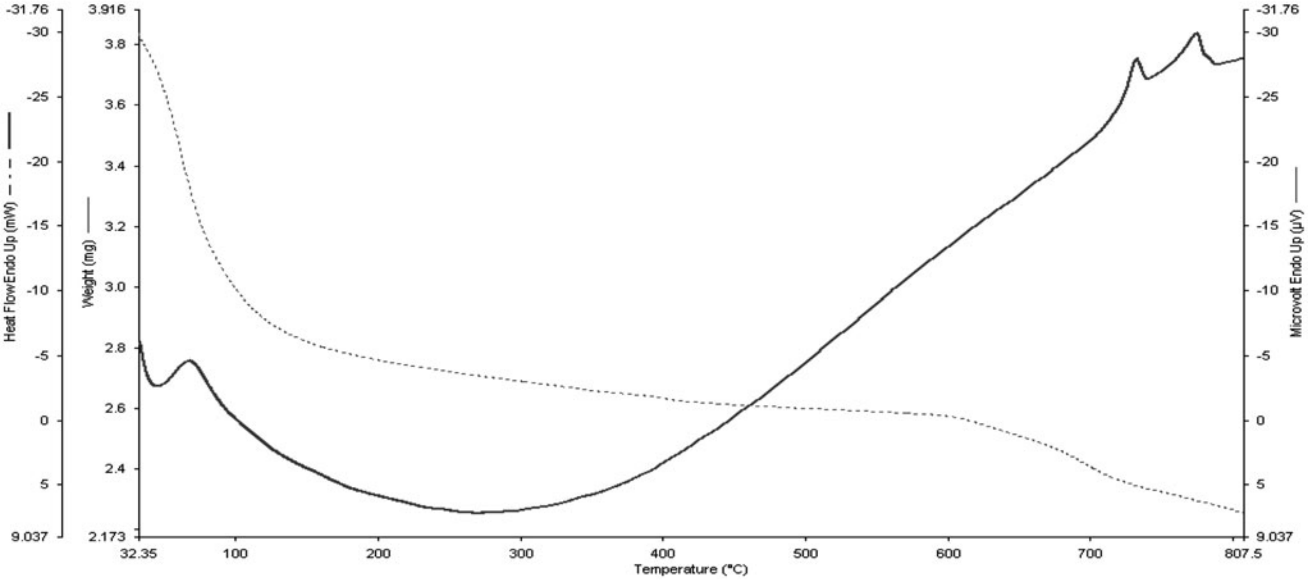

Fig. 1. Thermal analysis diagram of SbZP.

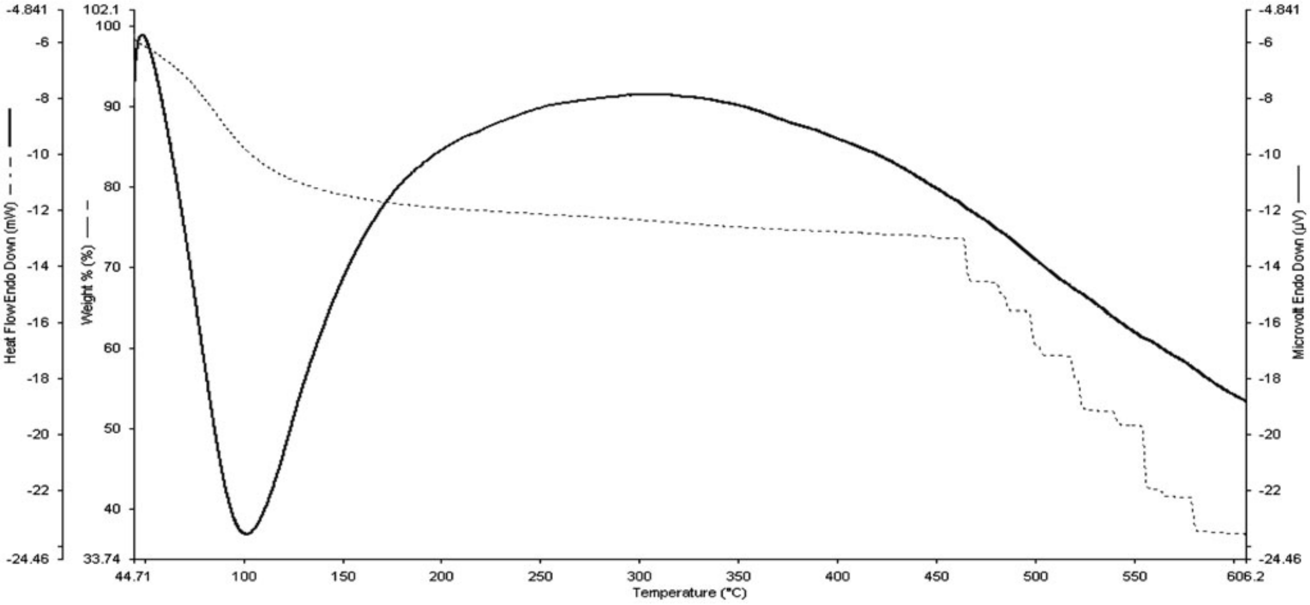

Fig. 2. Thermal analysis diagram of SbZP.

The effect of size and charge on ion-exchange capacity was studied for alkali and alkaline earth metal ions, and the order was found to be $Li^+ < Na^+ < K^+$; $Mg^{2+} < Ca^{2+} < Ba^{2+}$ confirming that ion exchange takes place with the hydrated form of the ions. The sodium-IEC decreases slightly with temperature, and the sample retained prominent capacity up to 500℃ and 400℃, respectively, for SbZP and SbZTP which can be explained with the obtained thermogram also. Distribution studies reveal the selectivity of the material towards various metal ions. For SbZP, it is in the order as follows: $Pb^{2+} > Hg^{2+} > Th^{4+} > Cu^{2+} > Al^{3+} > Ca^{2+} > Mg^{2+} > Y^{3+} > Zn^{2+} > Ni^{2+} > Co^{2+} > Mn^{2+}$, and for SbZTP, the order is $Pb^{2+} > Hg^{2+} > Th^{4+} > Co^{2+} > Cu^{2+} > Mn^{2+} > Cd^{2+} > Y^{3+} > Mg^{2+} > Ni^{2+} \approx Ca^{2+} \approx Zn^{2+}$ showing high selectivity towards toxic heavy metal ions such as Pb^{2+}, Hg^{2+} and Th^{4+}.

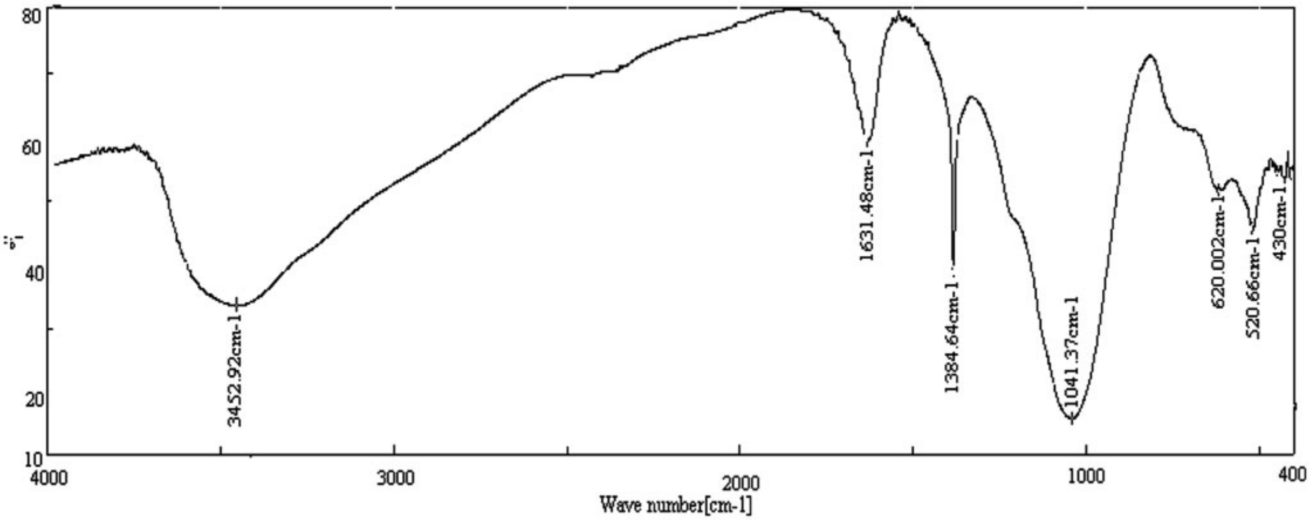

Fig. 3. FTIR of SbZP.

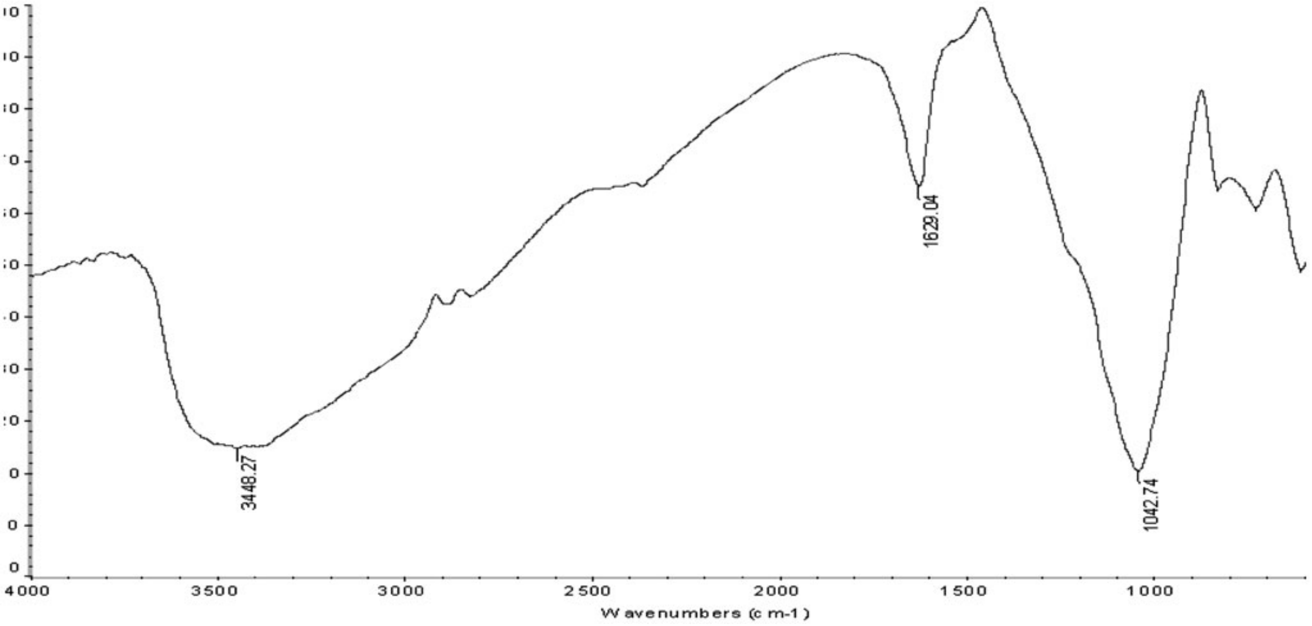

Fig. 4. FTIR of SbZTP.

3.2. Kinetic studies

The rate determining step in ion-exchange process is either particle diffusion or film diffusion which is not affected by agitation of the solution. Kinetics of ion-exchange can be explained with respect to fractional attainment of equilibrium $U_{(\tau)}$. For a particle diffusion controlled phenomenon [10],

$$U_{(\tau)} = \frac{\text{Amount of exchange at time } t}{\text{Amount of exchange at equilibrium}} = 1 - \left(\frac{Q_{\mathrm{H}}(t)}{Q^{\circ}_{\mathrm{H}}}\right) = \left[\frac{C_0 - C_{\mathrm{t}}}{C_{\mathrm{t}} - C_{\infty}}\right] \tag{2}$$

where Q_{H} (t) is the H^{+} ion content present at time t and Q°_{H} is the amount present initially in the ion exchanger, while C_t, C_∞ and C_o are concentrations of metal ions at time t, equilibrium concentration and initial concentration, respectively. $U_{(\tau)}$ is seen to be dependent only on the magnitude of the dimensionless time parameter, τ. For a particle diffusion controlled phenomenon, the numerical results can be expressed by the explicit approximation [11],

$$U_{(\tau)} = [1 - \exp\{\pi^2\ (f_1(\alpha)\tau + f_2(\alpha)\tau^2 + f_3(\alpha)\tau^3)\}]^{1/2} \tag{3}$$

where τ is half-time of exchange equal to $\bar{D}_H\ t/r_o^2$, mobility ratio, $\alpha = \bar{D}_H/\bar{D}_M$, r_o is the particle radius which is taken as 125×10^{-6} m (50–70 mesh) in the present study. $\bar{D}_M$ and $\bar{D}_H$ are the inter-diffusion coefficients of the metal ions and hydrogen ions, respectively, in the exchanger phase. The approach is based on Nernst–Planck equation [12]. The three functions $f_1(\alpha)$, $f_2(\alpha)$, and $f_3(\alpha)$ depend upon the mobility ratio (α) and the charge ratio (Z_H/Z_M) of the exchanging ions. Thus, they have different expressions as given below. When the exchanger is taken in the H^+ form and the exchanging ion is M^{2+}, for $1 \le \alpha \le 20$, as in the present case, the three functions have the values:

$$f_1(\alpha) = -\frac{1}{0.64 + 0.36\alpha^{0.668}} \tag{4}$$

$$f_2(\alpha) = -\frac{1}{0.96 + 2.0\alpha^{0.4635}} \tag{5}$$

$$f_3(\alpha) = -\frac{1}{0.27 + 0.096\alpha^{1.140}} \tag{6}$$

Each value of $U_{(\tau)}$ has a corresponding value of τ [13]. Straight lines passing through the origin in the τ vs. time (t) plots will confirm particle diffusion controlled phenomenon. Conditions favouring particle diffusion controlled ion exchange phenomenon are as follows: high metal ion concentration, relatively large particle size of the exchanger and vigorous shaking of the solution. So kinetic measurements were carried out

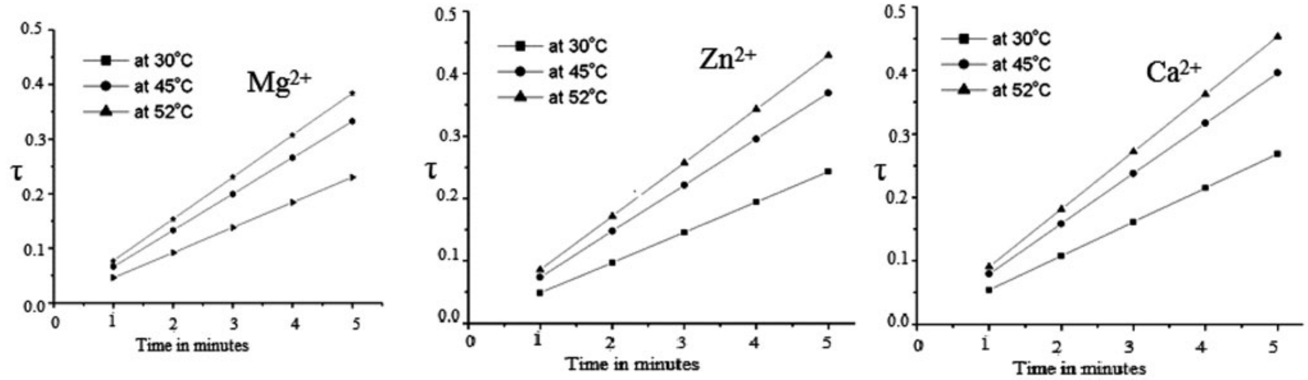

Fig. 5. τ vs. time plots of exchange of Mg^{2+}, Zn^{2+} and Ca^{2+} with H^+ at different temperatures on SbZP.

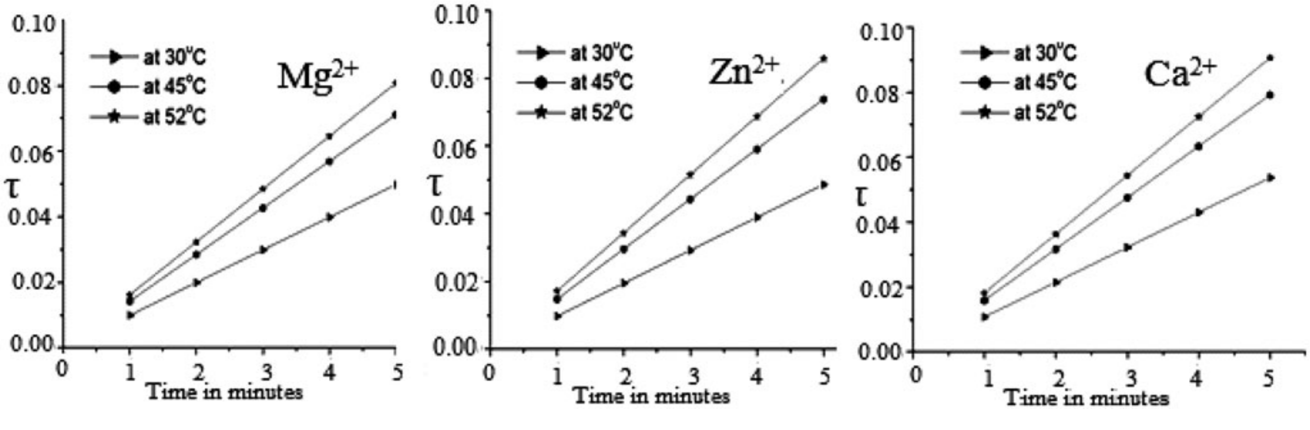

Fig. 6. τ vs. time plots of exchange of Mg^{2+}, Zn^{2+} and Ca^{2+} with H^+ at different temperatures on SbZTP.

Table 1
Slopes (S) of the τ vs. time plots for metal ions on SbZP

Migrating ions	Slope $(S) \times 10^4$ (s^{-1}) at temperature 30˚C	45˚C	52˚C
Mg^{2+}	1.53	2.22	2.56
Zn^{2+}	1.62	2.46	2.86
Ca^{2+}	1.79	2.64	3.02

Table 2
Slopes (S) of the τ vs. time plots for metal ions on SbZTP

Migrating ions	Slope $(S) \times 10^4$ (s^{-1}) at temperature 30˚C	45˚C	52˚C
Mg^{2+}	1.66	2.37	2.69
Zn^{2+}	1.74	2.57	3.01
Ca^{2+}	1.92	2.78	3.14

under this condition. The slopes of the lines are related to $\bar{D}_H$ as:

$$S = \bar{D}_H / r_\circ^2 \tag{7}$$

Straight lines in the plots of $-\log \bar{D}_H$ vs. $1/T$ will show the validity of Arrhenius equation:

$$\bar{D}_H = D_0 \exp(-E_a/RT) \tag{8}$$

The energy of activation, E_a, and the constant D_o can be evaluated from the slope and intercept of these plots. The entropy of activation, ΔS^*, was calculated using the equation:

$$D_0 = 2.72 \frac{d^2 kT}{h} \exp\left(\frac{\Delta s^*}{R}\right) \tag{9}$$

where d is the average distance between two exchanging sites taken as 5×10^{-10} m, k is the Boltzmann constant, R is the gas constant and h is the Planck's constant. T is taken as 273 K.

τ vs. time (t) plots for metal ion solutions of concentrations 0.002, 0.004, 0.006, 0.008 and 0.01 M were

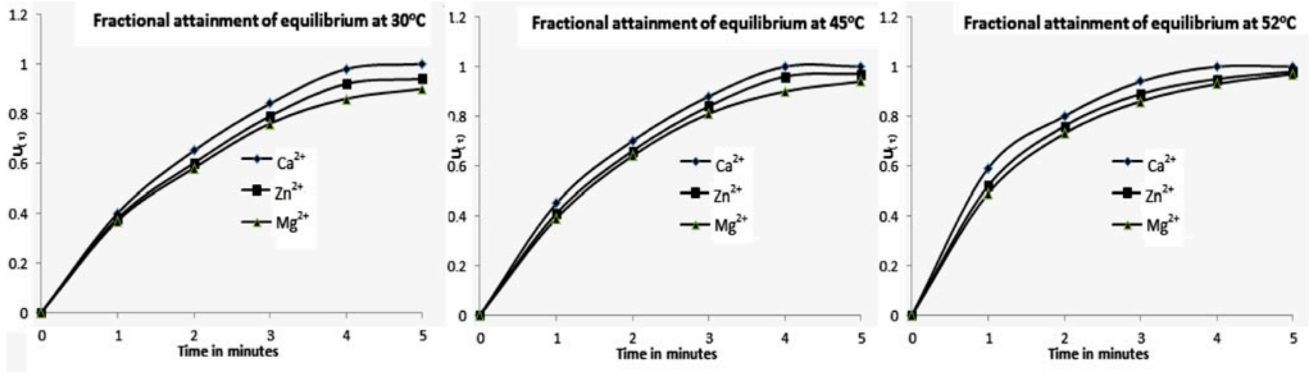

Fig. 7. Fractional attainment of equilibrium vs. time graph using SbZP.

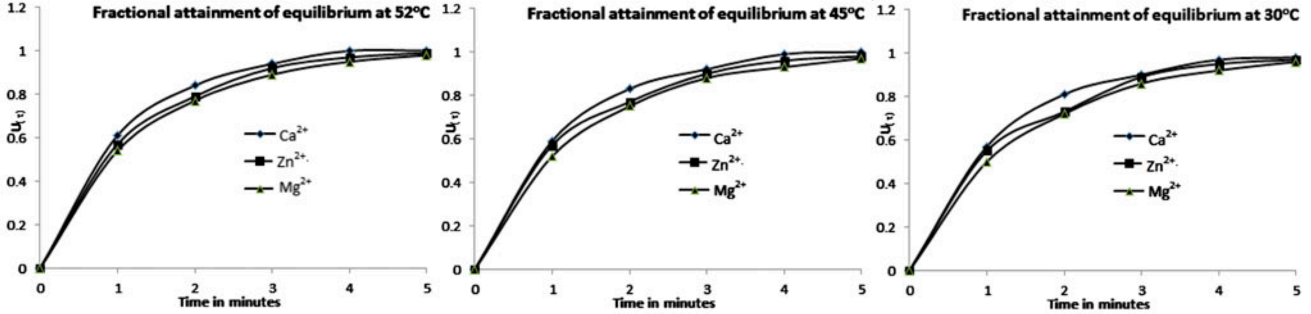

Fig. 8. Fractional attainment of equilibrium vs. time graph using SbZTP.

plotted to know the concentration of solution to be selected for the studies. It was found that τ vs. time (t) plots were straight lines passing through the origin in the case of metal ion solutions of concentrations greater than 0.008 M which confirms particle diffusion controlled phenomenon, below which film diffusion control phenomenon was prominent. So studies were conducted using 0.01 M of metal ion solutions.

The slopes (S) of various τ vs. time (t) plots (Figs. 5 and 6) for the three metal ions for the exchangers (Tables 1 and 2) indicate that the attainment of equilibrium is faster at a higher temperature, which suggests that the mobility of the ions increases with temperature (Figs. 7 and 8) which are related to $\bar{D}_H$ (Eq. (7)).

The plots of $-\ln \bar{D}_H$ vs. $1/T$ gave straight lines (Figs. 9 and 10), which show the validity of Arrhenius equation (Eq. (8)).

The values of slopes, D_o, E_a and ΔS^* are given in Tables 3 and 4.

ΔS^* is found to be negative in all cases showing decrease in degree of randomness at exchanger surface during ion-exchange process indicating increased selectivity to metal ions when the exchanger phase is in H^+ form and feasibility of metal ion exchange.

Overall rate of exchange reaction depends on D_o, E_a and ΔS^*. Low E_a values indicate that metal ion exchange studied herein is diffusion controlled.

Since D_o gives an idea about mobility of migrating ions, it therefore depends on size and charge of ion on the extent of hydration in aqueous medium. In the present study, order for D_o, E_a and ΔS^* is $Zn^{2+} > Mg^{2+} > Ca^{2+}$ which could not be related to ionic radii of metal ions. Other factors that contribute to D_o are electrostatic interaction of metal ions with exchange sites, which increases with increase in charge density, site acidity, pore size of exchanger particle, etc. which could be decisive factors in certain cases.

The two exchangers under study showed similar trend in kinetic parameters, D_o, E_a and ΔS^*. The higher

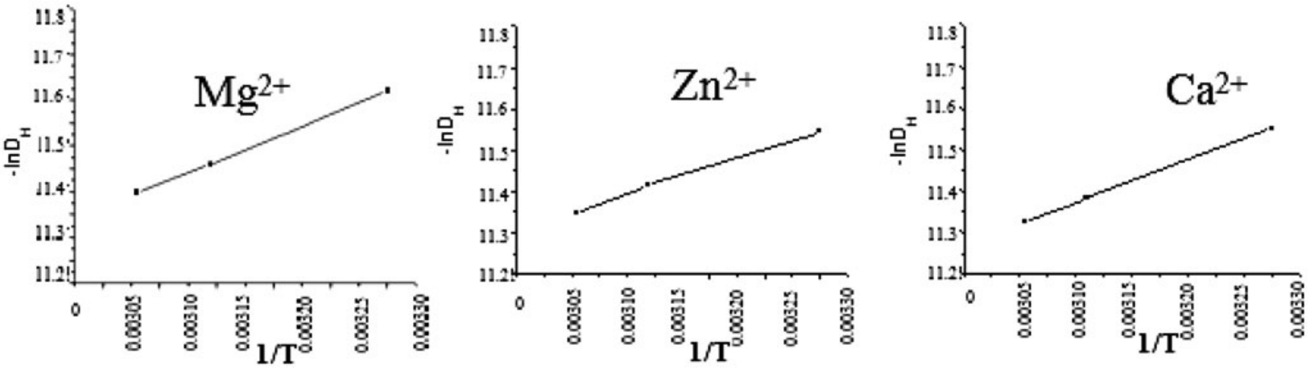

Fig. 9. Plots of $-\ln \bar{D}_H$ vs. $1/T$ for metal ions on SbZP.

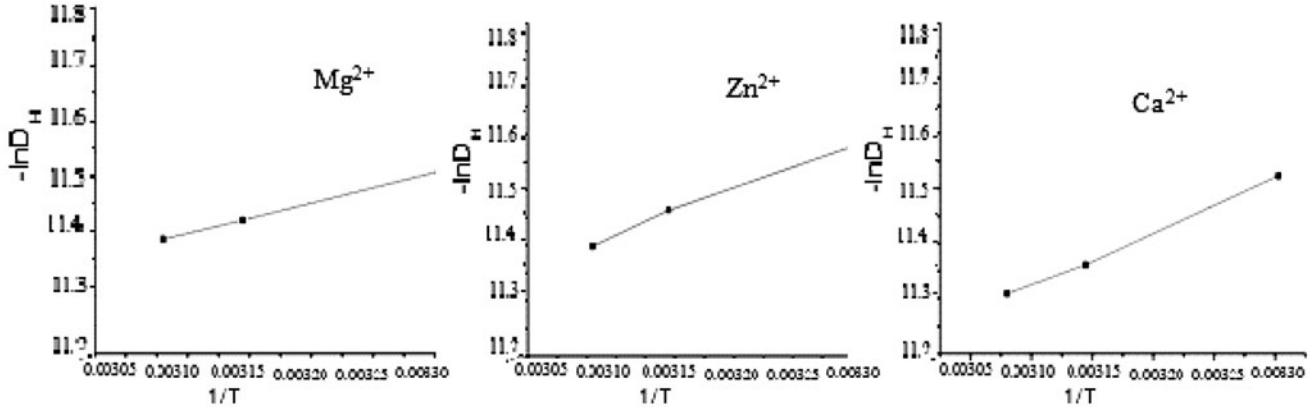

Fig. 10. Plots of $-\ln \bar{D}_H$ vs. $1/T$ for metal ions on SbZTP.

Table 3
D_o, E_o and ΔS^* for the exchange of metal ions on SbZP

Migrating ions	Ionic radii (A°)	D_o (m^2s^{-1})(10^{-9})	E_a (KJ mol^{-1})	ΔS^* (JK^{-1} mol^{-1})
Mg^{2+}	0.65	5.2	19.351	−54.97
Zn^{2+}	0.74	1.4	15.558	−65.88
Ca^{2+}	0.99	8.4	20.201	−50.99

Table 4
D_o, E_o and ΔS^* for the exchange of metal ions on SbZTP

Migrating ions	Ionic radii (A°)	D_o (m^2s^{-1})(10^{-9})	E_a (KJ mol^{-1})	ΔS^* (JK^{-1} mol^{-1})
Mg^{2+}	0.65	4.0	18.510	−57.13
Zn^{2+}	0.74	0.4	12.306	−76.30
Ca^{2+}	0.99	6.4	19.331	−53.25

IEC of SbZTP than that of SbZP explains the increased values obtained for SbZTP.

Ion-exchange kinetic studies on the materials revealed the mechanism of exchange to be particle diffusion. Activation energy is calculated using verified and validated Arrhenius equation. The negative values of ΔS^*indicate that the ion-exchange process by metal ions is feasible on the H^+ form of the material.

The kinetic measurements of different metal ions at a prescribed set of conditions formulate the energy of activation and entropy of activation involved in a particular ion-exchange reaction. These two state functions imply the value of enthalpy change for the reaction. That is the possibility of using an ion exchanger as selective scanner of ionic species in chemical reaction series may be predicted using the knowledge of these parameters and predict the feasibility of the ion exchanger to be used as a catalyst or inhibitor.

4. Conclusion

The ion exchangers synthesised were found to possess very good ion-exchange properties. They possess high selectivity towards heavy metal ions, Pb^{2+}, Hg^{2+} and Th^{3+}. They also possess relatively high surface areas. So the materials are promising in environmental chemistry. The kinetics of exchange of Mg^{2+}, Zn^{2+} and Ca^{2+} revealed the mechanism to be particle diffusion. Kinetic parameters such as pre-exponential constant (D_o), energy of activation (E_o) and entropy of activation (ΔS^*) have been evaluated. The negative values of ΔS^* indicate that the exchange process by metal ions is feasible on the H^+ form of the material. Thus, we can predict the feasibility of an ion-exchange process to be used as a catalyst or inhibitor.

Acknowledgement

One of the authors, Preetha B, acknowledges the University Grants Commission, India for the fellowship under FIP and STIC, Cochin, Kerala, for providing technical facilities.

References

[1] A. Jayswal, U. Chudasama, Sorption of Pb(II), Bi(III) and Th(IV) on zirconium phosphate, J. Sci. Ind. Res. 66 (2007) 945–951.

[2] A. Khan, A.M. Asiri, A.A.P. Khan, S.B. Khan, Electrical conductivity and ion-exchange kinetic studies of polythiophene Sn(VI)phosphate nano composite cation-exchanger, Arabian J. Chem. (2014), in press. doi: 10.1016/j.arabjc.2014.09.004.

[3] I.A. Stenina, A.D. Aliev, P.K. Dorhout, A.B. Yaroslavtsev, Cation mobility and kinetics of ion exchange in zirconium hydrogen monothiophosphate hydrate, $Zr(HPO_3S)_2{\cdot}1.5H_2O$, Inorg. Chem. 43 (2004) 7141–7145.

[4] A.S. Weqar, A.K. Shakeel, Synthesis, characterization and ion exchange properties of zirconium (IV) tungstoiodophosphate, a new cation exchanger, Bull. Mater. Sci. 30 (2007) 43–49.

[5] A. Zeid Al-Othman, Z. Al-Othman, Inamuddin, M. Naushad, Determination of ion-exchange kinetic parameters for the poly-o-methoxyaniline Zr(IV) molybdate composite cation-exchanger, Chem. Eng. J. 166(2) (2011) 639–645.

[6] A.I. Vogel, A Text Book of Quantitative Inorganic Analysis, Longman Group Limited, London, 1975 p. 490, 451 & 499.

[7] W.A. Siddiqui, S.A. Khan, Synthesis, characterization and ion exchange properties of zirconium(IV) tungstoiodophosphate, a new cation exchanger, Bull. Mater. Sci. 30(1) (2007) 43–49.

[8] E. Husson, The vibrational spectra of some antimony phosphates, J. Solid State Chem. 75 (1988) 305–312.

[9] P. Singh, J.P. Rawat, N. Rahman, Synthesis and characterization of zirconium(IV) iodovanadate and its use as electron exchanger, Talanta 59 (2003) 443–452.

[10] R.M. Barrer, Diffusion in and through Solids, Cambridge University Press, New York, NY, 1941, p. 29, 50.

[11] F. Helfferich, Ion Exchange, McGraw-Hill, New York, NY, 1962, p. 255, 282.

[12] M.S. Plesset, F. Helfferich, J.N. Franklin, Ion exchange kinetics: A nonlinear diffusion problem. II. Particle diffusion controlled exchange of univalent and bivalent ions, J. Chem. Phys. 29 (1958) 1064–1069.

[13] F.G. Helfferich, Ion Exchange, Dover Science, Mineola, NY, 1995, pp. 250–320.